PHYSICAL REVIEW E **76**, 045301(R) (2007)

Dynamics of thin liquid films falling on vertical cylindrical surfaces subjected to ultrasound forcing

Len Moldavsky, Mati Fichman, and Alexander Oron*
Department of Mechanical Engineering, Technion - Israel Institute of Technology, Haifa 32000, Israel
(Received 12 July 2007; published 19 October 2007)

Axial ultrasound forcing applied to a vertical cylinder is shown to affect a gravity-driven flow of a thin liquid film on its outer surface. In the case of larger forcing amplitudes, we find that the film flow can be completely stopped.

DOI: 10.1103/PhysRevE.76.045301 PACS number(s): 47.15.gm, 47.85.mb

Flows of falling liquid films on vertical cylindrical surfaces have been investigated for several decades mainly motivated by technological applications of cooling solid columns by running liquids. The system also represents a paradigm for developing various theories suitable for investigation of nonlinear dynamics of the films that exhibit an intricate behavior of interfacial waves changing in both space and time.

Kapitza and Kapitza [1] were the first to carry out experiments with film flows on a vertical cylindrical surface and to document their results. They reported the emergence of periodic and solitary waves in the free and forced regimes. Binnie [2] carried out experiments with falling films on a cylinder and found spiral waves. Alekseenko *et al.* [3,4] performed extensive experimental studies with falling films on vertical cylindrical surfaces and the emergence of spatially and temporally periodic and aperiodic wave regimes was reported in the cases of both natural and upstream perturbed flows. Kliakhandler *et al.* [5] found in their experiments three distinct regimes, namely, (i) at relatively large flow rates, the pattern that consists of large and fast moving droplets with large separation distance; (ii) in the narrow interim range of flow rates, a periodically organized pattern that consists of much smaller and slower moving than in (i) droplets; (iii) at very low flow rates, an irregular pattern of larger than in (ii) but smaller than in (i) droplets with large and spatially nonuniform spacing between them that collide and merge with the smaller droplets ahead and as a result move with a time-periodic speed. Craster and Matar [6] conducted experimental studies of film flow on a vertical cylinder and observed, in contrast to Kliakhandler *et al.* [5], a gradual transition of patterns with a decrease of the flow rate from the periodic nearly-spaced stationary wave train to the widely spaced pattern of time-varying droplet structure.

Linear stability analysis of the unperturbed flow on a vertical cylinder was carried out by several authors [7–9]. Absolute and convective instabilities in falling films on a vertical cylinder were studied theoretically and experimentally [10,11]. Various nonlinear model equations were developed to investigate the dynamics of thin liquid films falling on a vertical cylindrical surface theoretically. These include the derivation of simplified evolution equations using various asymptotic methods and their analytical and numerical investigation. These evolution equations may be single weakly nonlinear [10,12,13], single strongly nonlinear [5,6,14–16], or may consist of a set of coupled evolution equations [17–19].

Small-amplitude–high-frequency vibration of various mechanical systems was shown to lead to striking results. One of the examples of such effects is the Kapitza pendulum [20], which exhibits an inverted pendulum with a vertically vibrating support. As a result of vibration, the upward equilibrium point unstable in the case of an unforced pendulum, becomes stable. Another example of a spectacular impact of vibration is the Chelomei's pendulum [21] which displays the configuration of the Kapitza pendulum equipped with a body sliding on the pendulum rod. As a result of vibration, the slider is stabilized and floats against gravity.

The purpose of this paper is to report the experimental results showing a dramatic change of the dynamics of a thin liquid film falling on a cylindrical surface subjected to small-amplitude ultrasound forcing.

A schematic of the experimental setup is shown in Fig. 1. A vertical stainless steel rod of length $L=50$ cm and diameter $d=0.2$ cm is welded to a bolt screwed into an ultrasound generator VCX-600 at its lower end, while at its upper end a concentric liquid reservoir is mounted. The gap between the rod surface and the inner surface of the dispenser at its opening through which a liquid flow is enabled is $h_0=0.025$ cm. The liquid used in our experiments is glycerol 93%, whose material properties are density $\rho=1126.0$ kg/m^3, dynamic viscosity $\mu=0.44$ kg/(m s), and surface tension $\sigma=0.064$ kg/s^2. As glycerol is known to be a hygroscopic liquid whose properties change significantly with the time of exposure, to the ambient air, we do not use it continuously for more than 120 minutes in the experiments, and we replace it with a fresh liquid afterwards. The volumetric flow rate is measured by monitoring the level change of the liquid in the upper reservoir, and the speed of droplets along the rod are measured by computerized postprocessing of the droplet location relative to the fixed scale. The ultrasound forcing is applied to the rod from below when the forcing frequency was fixed at $\Omega=20$ kHz. The maximal output of the generator is 600 W and the amplitude of the forcing is possible to control within the range of $0<a<124$ μm. The experiments are carried out in an air-conditioned chamber with the temperature held at 22 °C. We also measure the apparent leading and trailing contact angles of the emerging droplets.

*meroron@tx.technion.ac.il

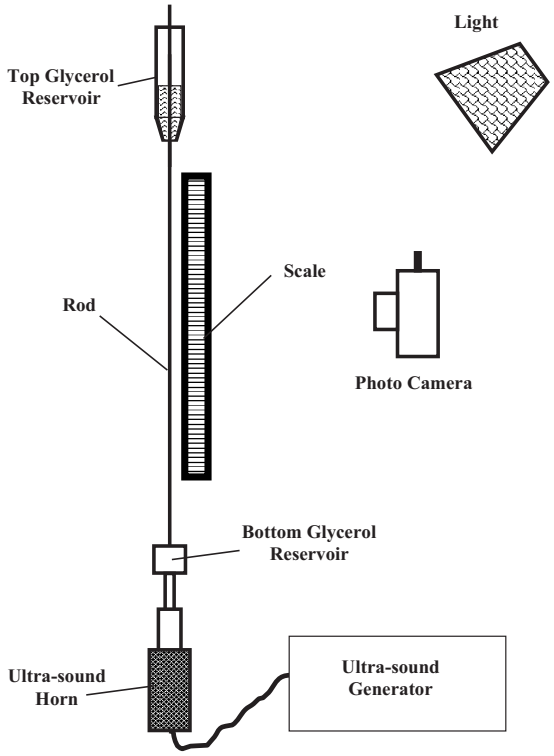

FIG. 1. Schematic of the experimental setup.

To calibrate our experimental system, the experiments are first carried out with an unforced system where an initially flat glycerol film of the thickness 0.25 mm at the point of inception flows on a static rod. The volumetric flow rate is measured to be $Q=2.5\times10^{-2}$ cm^3/s and the Reynolds number based on the maximal fluid velocity obtained from the exact solution of the Navier-Stokes equations for an axisymmetric film of a uniform thickness h_0 on a cylindrical surface of diameter d, e.g. [5,6],

$$R=\frac{\rho^2 g h_0^3}{4\mu^2}\left[2\left(1+\frac{d}{2h_0}\right)^2\ln\left(1+\frac{2h_0}{d}\right)-1-\frac{d}{h_0}\right], \quad (1)$$

is estimated to be 6.0×10^{-4}. Note that the maximal velocity in the film is given by

$$u_m=\frac{\rho g h_0^2}{4\mu}\left[2\left(1+\frac{d}{2h_0}\right)^2\ln\left(1+\frac{2h_0}{d}\right)-1-\frac{d}{h_0}\right].$$

The estimated average flow velocity in the film is given by $u_{av}=4Q/\{\pi[(d+h_0)^2-d^2]\}$ is 1.4 cm/s. The measurements of the droplet speed shows the average value of 1 cm/s. The pattern consisting of traveling droplets is shown in the left panel of Fig. 2. The pattern of droplets with spacing along the rod varying within the range of 1 cm $<L_n<$2.5 cm emerges downstream, which is in good agreement with the linear stability analysis of Craster and Matar [6]. Indeed, their theory gives the nondimensional fastest growing wave number scaled with the capillary length $\mathcal{L}=2\sigma/(\rho g d)$, as $k_m=\sqrt{2}\mathcal{L}/d$. The wavelength corresponding to this value of k_m is obtained for our experiment as $l=0.9$ cm. The difference between the theory [6] and our experiments arises from the fact that the theory assumes axisymmetric flow, while in the experiments such symmetry was lost.

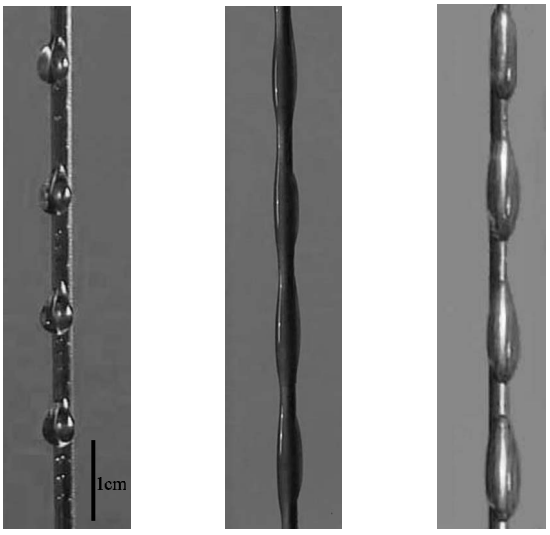

FIG. 2. The photographs of the droplet patterns obtained at different levels of forcing. Left panel: unforced system, $a=0$, traveling droplets; middle panel: forced system with $a=75$ μm, static droplets; right panel: forced system with 100 μm, static droplets.

Loss of axial symmetry of the flow in our experiments with respect to other experimental observations may be explained in the following way. In our experiments, the ratio between the mean thickness of the liquid film h_0 and the rod diameter d is $H\equiv h_0/d=0.125$. In the experiments conducted by Craster and Matar [6] and Kliakhandler *et al.* [5], the value of H ranged between 1.5 and 2.5, i.e., an order of magnitude higher. At the same time, the densities and dynamic viscosities of glycerol used in the present work, castor oil [5] and silicone oil 500 cS [6], are similar, while the values of surface tension for these liquids are, respectively, $\sigma_{GL}=64.0$ g/s^2, $\sigma_{CO}=31.0$ g/s^2, and $\sigma_{SO}=20.4$ g/s^2. We conclude that the dominant factor for loss of axial symmetry of the flow is the geometrical one, h_0/d. We have also carried out a series of experiments with several liquids of surface tension lower than that of glycerol, such as ethanol and liquid soap, with the experimental setup of the unforced system remaining unchanged. These films retained their axial symmetry. Based on these facts, we conjecture that thinner falling films of liquids with higher surface tension tend to be apter to lose their axial symmetry.

In the forced regime, we found several distinct regimes. When the amplitude of forcing is below 60 μm, the speed of the droplets slightly decreases and their shapes and the spacing between them slightly change. An increase of the forcing amplitude into the interval 60 μm$<a<$75 μm leads to a significant slow down of the droplets' speed in the lower part of the rod and to a slip-stick motion in the upper part of the rod. The latter consists of a slow increase of a droplet size fed by the flow from the upper reservoir and a fast draining of the liquid from the droplet into the one right below it. This process repeats for several minutes.

When the amplitude of forcing reaches into the interval 75 μm$<a<$100 μm, the flow in the film stops completely,

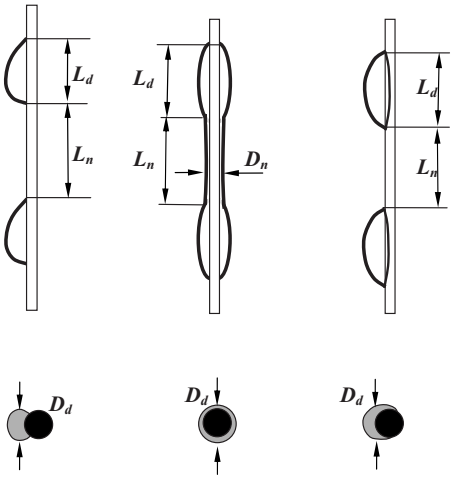

FIG. 3. Schematic of the droplets topology and definition of geometric properties of the droplets. In the upper row: left panel—unforced system, $a=0$; middle panel—forced system with $a=75$ μm; right panel—forced system with $a=100$ μm. The lower row shows configurations of the droplets (gray) with respect to the rod (black).

as shown in the middle panel of Fig. 2. This result is ascertained by monitoring the level of the liquid in the upper reservoir. An increase of the forcing amplitude even further into the domain of $a \geqslant 100$ μm leads to the change of the droplets' shape and to the emergence of apparently isolated beads separated by ultrathin liquid bridges of thickness below 10 μm, as shown in the right panel of Fig. 2. The flow in the film remains halted. The droplets in both of the configurations shown in the middle and right panels of Fig. 2 are visibly static, although one cannot rule out that they are entrained in small-amplitude fast vertical oscillations.

Measurements of the apparent leading and trailing contact angles between the droplets and the rod show that in the case of an unforced system, they vary along the rod in the range between 45° and 10°. The shape of the droplets changes with the forcing amplitude. As seen in Fig. 2 and shown in Fig. 3, the droplets' shape in a free (unforced) system is strongly asymmetric with a bulge pointing downward. Forcing of the film with the amplitude $a=75$ μm leads to the situation in which the contact angles are within the range between 8° and 10° with no visible difference between the two. Forcing of the system with $a=100$ μm causes the leading contact angle to increase into the domain between 30° and 45°, while the trailing contact angle remains between 8° and 10°. Table I contains a summary of the measured geometrical properties.

A sketch showing the structure of the droplet patterns in the unforced system and the forced system at two different values of forcing amplitude of $a=75$ μm and $a=100$ μm is given in Fig. 3. The droplets have a tendency to fall on a side of the rod and not to preserve an axisymmetric shape. An

TABLE I. Measured geometrical properties of the droplet pattern for the unforced system and various levels of forcing.

	$a=0$	$a=75$ μm	$a=100$ μm
D_d (cm)	0.5	0.5	0.4
D_n (cm)	0.25	0.22	0.2
L_d (cm)	0.5–0.8	0.8	0.7
L_n (cm)	1.0	0.5	0.3

increase of the forcing amplitude causes a symmetrization of the droplets in both up-down and circumferential direction. The typical diameter D_d of the droplets decreases with it. Both the diameter and the length of the neck D_n and L_n, respectively, decrease with an increase of a. A further increase of the forcing amplitude to $a=100$ μm leads to the symmetry break again.

To verify the robustness of the results with respect to the direction of ultrasound forcing, we repeated the series of experiments with the ultrasound horn being attached to the upper end of the rod. Several series of experiments with significantly lower forcing frequencies (~20–30 Hz) were also carried out with larger forcing amplitudes. In all of these, the phenomenon of the flow cessation persists. A set of experiments with ultrasound forcing of a horizontal rod coated with a liquid film was performed as well. In the case of the unforced system, pendant drops emerge on the underside of the rod. However, forcing of a rod results in patterns similar to that shown in the middle panel of Fig. 2 and in prevention of dripping. These results are outside the scope of this paper and will be discussed elsewhere.

A theoretical study of the phenomena reported here is underway. The influence of parametric excitation imparted by in-plane wall oscillation on falling liquid films down a vertical wall was previously studied in the framework of linear stability theory [22,23] and nonlinear theories [24–26]. These studies showed the emergence of windows of film stabilization in terms of a decrease of the wave amplitude, but this stabilization does not lead to flow halt. On the other hand, stabilization of the Chelomei's pendulum whose configuration resembles to some extent that of the droplets sliding along the forced vertical rod, was shown to be due to small-amplitude flexural vibrations of the rod [27]. A similar effect may be responsible for a complete cessation of a flow reported here.

In summary, we report the dramatic change in the properties of a thin film flow on a vertical cylindrical surface subjected to ultrasound axial forcing. Variation of the vibration amplitude leads to the possibility of a flow control including the flow rate. An increase of the forcing amplitude causes the flow in a film to come to a complete stop.

The research was partially supported by the Technion President Fund and the Fund for Promotion of Research at the Technion.

[1] P. L. Kapitza and S. P. Kapitza, Zh. Eksp. Teor. Fiz. **19**, 105 (1949).
[2] A. M. Binnie, J. Fluid Mech. **2**, 554 (1957).
[3] S. V. Alekseenko, V. Ya. Nakoryakov, and B. G. Pokusaev, AIChE J. **31**, 1446 (1985).
[4] S. V. Alekseenko, V. E. Nakoryakov, and B. G. Pokusaev, *Wave Flow in Liquid Films* (Begell House, New York, 1994).
[5] I. L. Kliakhandler, S. H. Davis, and S. G. Bankoff, J. Fluid Mech. **429**, 381 (2001).
[6] R. V. Craster and O. K. Matar, J. Fluid Mech. **553**, 85 (2006).
[7] S. L. Goren, J. Fluid Mech. **12**, 309 (1962).
[8] W. B. Krantz and R. L. Zollars, AIChE J. **22**, 930 (1976).
[9] F. J. Solorio and M. Sen, J. Fluid Mech. **187**, 365 (1987).
[10] R. J. Deissler, A. Oron, and Y. C. Lee, Phys. Rev. A **43**, 4558 (1991).
[11] C. Duprat, C. Ruyer-Quil, S. Kalliadasis, and F. Giorgiutti-Dauphiné, Phys. Rev. Lett. **98**, 244502 (2007).
[12] S. P. Lin and W. C. Liu, AIChE J. **21**, 775 (1975).
[13] T. Shlang and G. I. Sivashinsky, J. Phys. (Paris) **43**, 459 (1982).
[14] P. Rosenau and A. Oron, Phys. Fluids A **1**, 1763 (1989).
[15] A. L. Frenkel, Europhys. Lett. **18**, 583 (1992).
[16] H.-C. Chang and E. A. Demekhin, J. Fluid Mech. **380**, 233 (1999).
[17] Y. Y. Trifonov, AIChE J. **38**, 821 (1992).
[18] S. Kalliadasis and H.-C. Chang, J. Fluid Mech. **261**, 135 (1994).
[19] G. M. Sisoev, R. V. Craster, O. K. Matar, and S. V. Gerasimov, Chem. Eng. Sci. **61**, 7279 (2005).
[20] P. L. Kapitza, Zh. Eksp. Teor. Fiz. **21**, 588 (1951).
[21] V. N. Chelomei, Sov. Phys. Dokl. **28**, 387 (1983).
[22] R. J. Bauer and C. H. von Kerczek, ASME Trans. J. Appl. Mech. **58**, 278 (1991).
[23] S. P. Lin, J. N. Chen, and D. R. Woods, Phys. Fluids **8**, 3247 (1996).
[24] A. Oron and O. Gottlieb, Phys. Fluids **14**, 2622 (2002).
[25] O. Gottlieb and A. Oron, Int. J. Bifurcation Chaos Appl. Sci. Eng. **14**, 4417 (2004).
[26] A. Oron, O. Gottlieb and E. Novbari (unpublished). Also, E. Novbari, M. Sc. thesis, Technion–Israel Institute of Technology, Haifa, Israel, 2006.
[27] J. J. Thomsen and D. M. Tcherniak, Proc. R. Soc. London, Ser. A **457**, 1889 (2001).